Studies on the phase transitions and properties of tungsten (VI) oxide nanoparticles by X-Ray diffraction (XRD) and thermal analysis

S.F. Abdullah[a,*], S. Radiman[b], M.A. Abdul Hamid[b] and N.B. Ibrahim[b]

[a]*Department of Engineering Science and Mathematics, College of Engineering, Universiti Tenaga Nasional, Km 7, Jalan Kajang-Puchong, 43009 Kajang, Selangor, Malaysia*
* Corresponding author. Tel.:+60-3-89287260; fax: +60-3-89212065
E-mail address: siti@uniten.edu.my (Siti Fazlili Abdullah)
[b]*School of Applied Physics, Faculty Science and Technology, University Kebangsaan Malaysia, 43600 Bangi, Selangor, Malaysia*

Tungsten (VI) oxide, WO_3 nanoparticles were synthesized by colloidal gas aphrons (CGAs) technique. The resultant WO_3 nanoparticles were characterized by thermogravimetric-differential thermal analysis (TG-DTA) and X-Ray diffraction (XRD) measurements in order to determine the phase transitions, the crystallinity and the size of the WO_3 nanoparticles. As a comparison, transmission electron microscope (TEM) was used to investigate the size of the WO_3 nanoparticles. The result from XRD and DTA show that the formation of polymorphs WO_3 nanoparticles have the following sequence: orthorhombic (β-WO_3) $\rightarrow$ monoclinic (γ-WO_3) $\rightarrow$ triclinic (δ-WO_3) $\rightarrow$ monoclinic (ε-WO_3) with respect to the calcination temperature of 400, 500, 600 and 700°C. No diffraction peaks were found in the X-Ray diffraction measurements for the sample heat treated at 300°C (as-prepared), suggesting that an amorphous structure was obtained at this temperature whereas the crystallinity had been obtained by the other samples of the WO_3 nanoparticles at the calcination temperatures of 400, 500, 600 and 700°C. It is also found that the X-Ray diffraction measurements produced an average diameter of (30 ± 5), (50 ± 5), (150 ± 10) and (200 ± 10) nm at calcination temperatures of 400, 500, 600 and 700°C respectively by using Debye-Scherrer formula. The TG curve revealed that the WO_3 nanoparticles is purely anhydrous since the weight loss is insignificant $(0.3 - 1.4)$ % from 30 until 600°C for the WO_3 nanoparticles calcined at 400°C. Finally, the composition and the purity of the WO_3 nanoparticles have been examined by X-Ray photoelectron spectroscopy (XPS). The results indicate no significant changes to the composition and the purity of the WO_3 nanoparticle produced due to the temperature variations.

I. INTRODUCTION

WO_3 nanoparticles had recently receiving a lot of attention because of their important applications such as in catalysis [1], surface acoustic wave gas sensor [2,] and detecting of hazardous pollutants such as NO_x [3] , H_2S [4] and other alcohol gases, for example CH_x, CO, and NH_3 [5-7]. The chemical and physical properties of metal oxides nanoparticles, including WO_3 nanoparticles are generally dependent on the route of their synthesis [8-10]. There are many techniques that have been developed for the preparation of nanoparticles, which include microemulsions [11], laser ablation [12], sol-gel [13], UV irradiation [14] and solvothermal process [15]. In the present work we have focused on the CGA technique to produce WO_3 nanoparticles. CGA method was used in order to template WO_3

nanoparticles. CGA are surfactant gas micro bubbles of 10-100 μm in diameter produced by a high intensity stirring (4000–10000 rpm) in a vessel of a surfactant solution composed of a gaseous inner core surrounded by a thin surfactant film. These bubbles, due to their small size, exhibit some colloidal properties as described by Sebba [16]. Such CGA system as shown schematically in Fig. 1 can form a suitable template for the formation of the nanoparticles.

This paper is the further studies from my previous paper [17]. In this study, the phase transitions of WO_3 nanoparticles due to temperature variations have been studied, using X-Ray diffraction measurements. The sequence of temperature-induced phase transitions from lower to higher temperature for nanocrystallized WO_3 is the following: orthorhombic (β-WO_3) $\rightarrow$ monoclinic (γ-WO_3) $\rightarrow$ triclinic (δ-WO_3) $\rightarrow$ monoclinic (ε-WO_3) (refer to Table 1) which is consistent with the reported by others in Ref. [18-22].

TABLE I. Size and phase structure of WO_3 nanoparticles at various calcination temperature as obtained from XRD and TEM

Temperature (°C)	Phase Structure	Size (nm) XRD	Size (nm) TEM
As-prepared	-	-	30-45
400	Orthorhombic	(30 ± 5)	35-65
500	Monoclinic	(50 ± 5)	60-80
600	Anorthic (triclinic)	(150 ± 10)	170-185
700	Monoclinic	(200 ± 10)	220-240

II. MATERIALS AND METHOD

IIa. Materials

Sodium sulfite (Na_2SO_3, 98%, SigmaUltra) and inorganic tungsten compound, sodium tungstate dihydrate ($Na_2WO_4 \cdot 2H_2O$) were purchased from Sigma-Aldrich.
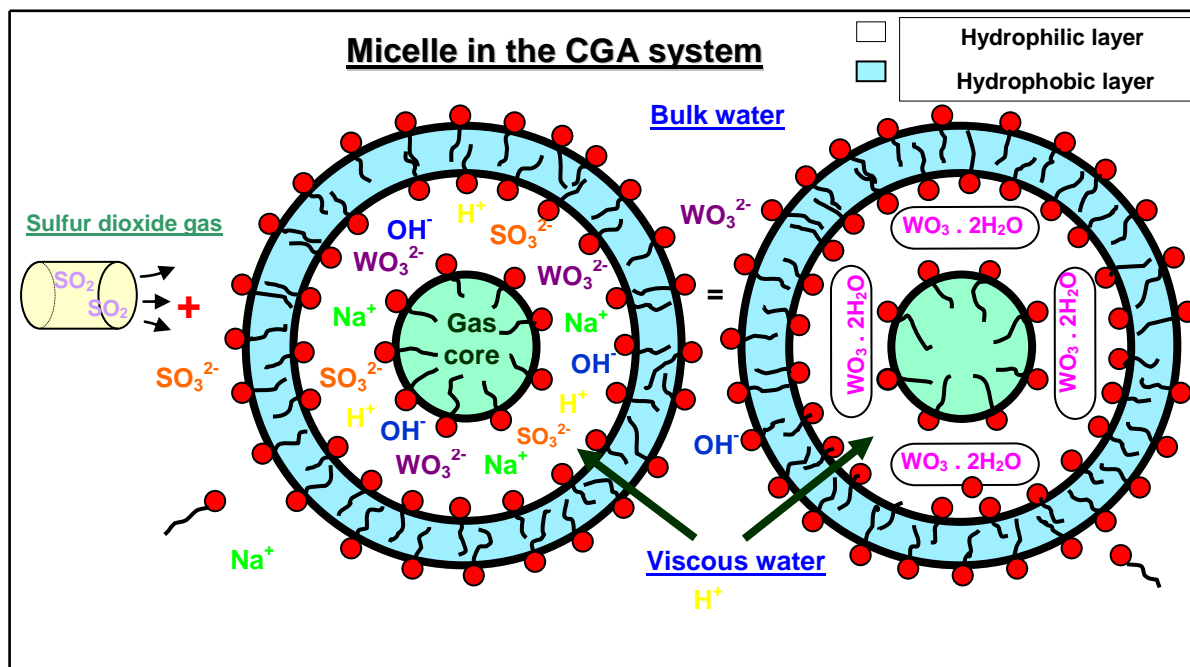
FIG. 1. A schematic flow chart of CGA technique for the synthesis of $WO_3 \cdot 2H_2O$.

Alkyl polyglucosides (commercially known as Glucopone 650 EC Solution, 65%) was supplied from Fluka whereas hydrochloric acid (37%) and ethanol (99.8%) were both obtained from Scharlau. Double-distilled and deionized water (Purelab Prima Elga, having 18.2 MΩ electrical resistivity) was used throughout the samples preparation. All the chemicals and solvents were of analytical purity and were used as received without further purifications.

IIb. Preparation of WO₃ Nanoparticles

The solution which consisted of Glucopone (60% wt. in water) was prepared. A 10.0 g of sodium tungstate dihydrate was then added to the solution. Finally, the CGAs system was produced by stirring at 13500 rpm using a high speed stirrer (M. Zipper GmbH D-7813 Staufen, model X 620 CAT). All preparations were carried out at temperature of 28°C. This method is described in Ref. [17]. The solutions which contain the precipitate were washed with deionized water and pure ethanol before centrifugation at 4000 rpm in order to remove the surfactant, residual reactants and other byproducts. This process was repeated at least five times. Finally, the resultant product was heated in a furnace at 300°C, for 3 h in order to remove water molecules from tungsten (VI) oxide dihydrate ($WO_3 \cdot 2H_2O$) to the anhydride (WO_3). The temperature at 300°C was chosen as the high peak started to appear from the XRD spectrum. This is followed by calcination for 4 h at four different temperatures, i.e., 400, 500, 600 and 700°C.

IIc. Characterization

The TG-DTA measurements were done on a Seiko 220U Thermogravimetry system with the temperature programming software of the furnace. The purge gas was N_2, supplied at a constant rate of 400 mL/min.

The sample weight loss (TG signal) and the energy loss (DTA signal) as functions of time and temperature were recorded continuously under dynamics conditions in the range of 30 - 600°C for the temperature measurements. In this investigation, TG-DTA data were used to determine the thermal decomposition, crystallization temperature which was found to be about 300° C and the effect of phase transitions of the samples.

Pyrolysis was carried out non-isothermally using 10.672 mg of WO_3 nanoparticles with the average size of (60 ± 5) nm placed in the platinum crucible which was then put on the sample pan hanging down in the reaction tube, in which the atmosphere could be controlled. The furnace tube was then raised to close the system. The pre-programmed control-unit regulates all the automatic functions of the recorder (e.g. the continuous change in the mass of the sample is measured), as well as the temperature programming of the furnace. After the furnace temperature had achieved its set value, the sample was allowed to cool slowly to room-temperature.

The X-Ray diffraction (XRD) measurements were performed by a Bruker X-Ray diffractometer at a scanning rate of 1°/min in the range of 10-70°, using a monochromatized Cu Kα radiation (λ = 0.154 nm). The silicon standard peak (111) was used to evaluate the instrumental broadening.

The X-ray photoelectron spectroscopy (XPS) was carried out by a Kratos XSAM X-ray photoelectron spectrometer having a base pressure of 10^{-9} Torr. The Mg Kα X-radiation was used as the excitation source. The binding energy of C1s (284.5 eV) was used as the reference in order to correct any charging shifts. A linear background subtraction has performed and the peaks in each spectrum were fit using a mixed Gaussian-Lorentzian function.

III. RESULTS AND DISCUSSION

The TG curve in Fig. 2 shows that the sample is purely anhydrous since the weight loss is insignificant 0.3–1.4 % from 30 up to about 300°C with almost no further weight loss observed until 600°C. The line (almost plateau) formed between 300 and 600°C on the TG curve indicates the formation of nanocrystalline WO_3 as decomposition product, as confirmed by XRD in Fig. 3. The DTA curves of thermal decomposition of WO_3 nanoparticles calcined at 400°C was shown in Fig. 2, a wide exothermic effect was observed with a peak at about 440°C, indicating that some phase transitions occurred which is from orthorhombic (β-WO_3) to monoclinic (γ-WO_3) as identified in ref. [23] and [24]. The DTA curve for the others calcination temperature which is 500, 600 and 700°C were not shown since they gave a consistent phase transitions that is from monoclinic (γ-WO_3) → triclinic (δ-WO_3), triclinic (δ-WO_3) → monoclinic (ε-WO_3) and monoclinic (ε-WO_3) (only) respectively as can be referred in Ref. [23-26].
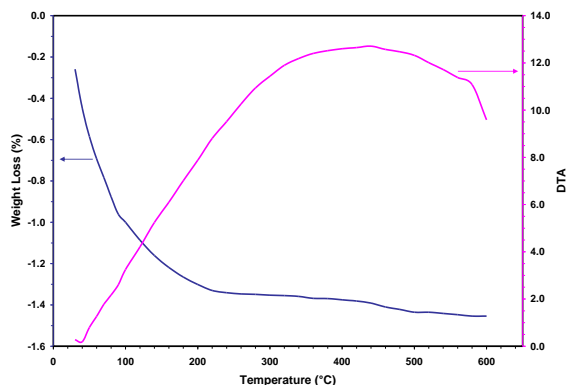
FIG. 2. The TG-DTA curves of thermal decomposition of WO_3 nanoparticles calcined at 400°C.
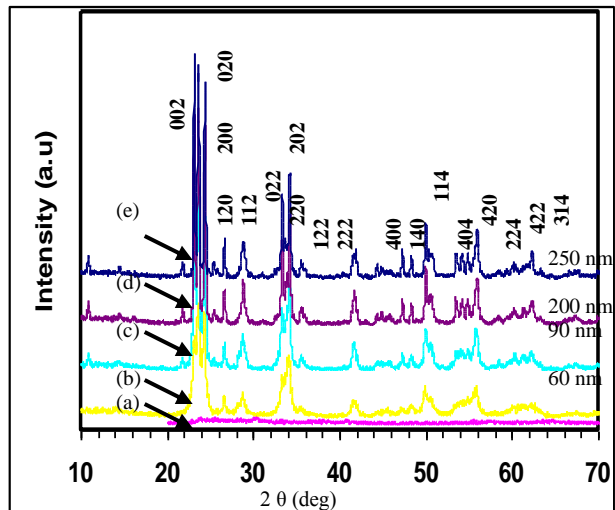
FIG. 3. The powder XRD patterns of WO_3 nanoparticles at various temperature: (a) as-prepared, (b) 400°C, (c) 500°C, (d) 600°C, (e) 700°C

The X-ray diffraction (XRD) patterns of the WO_3 are depicted in Fig. 3. The spectrum presents twenty-two broaden peaks at about 23.1, 23.6, 24.4, 26.5, 28.6, 33.2, 34.0, 34.2, 35.3, 41.4, 49.6, 49.7, 49.7, 50.1, 50.2, 55.3, 55.4, 55.6, 59.1, 60.9, 60.9 and 62.3° in 2θ, which correspond to the Miller index of the reflecting planes for (002), (020), (200), (120), (112), (022), (202), (220), (122), (222), (400), (140), (232), (114),(322), (402), (142),(420), (224), (422), (015) and (314) respectively. All peaks could be indexed to the standard patterns reported by the Joint Committee on Powder Diffraction Standards (JCPDS) [23-26], indicating a very high purity of the powder in all cases. It shows that all the calcined WO_3 produced are in crystalline form whereas as-prepared WO_3 nanoparticles are in amorphous form.

The average crystallite sizes of the nanoparticles can be obtained from the full-width half-maximum (FWHM) of the diffraction peaks by using Debye-Scherrer formula [27].

$D = (0.89 \lambda) / (B \cos \theta)$, where D is the diameter of the crystallites, 0.89 is the shape factor, λ is the X-Ray wavelength, B is the

breadth of the diffraction lines in radian and θ is the diffraction angle in degree. The reflecting peak at the crystal planes of (0 0 2) for all the samples is chosen to estimate the average size of the nanocrystals.

Table 1 shows the phase transitions and the size with respect to the various calcination temperature [28 – 33]. Besides that the size of the WO_3 particles with TEM observation is compared [17]. Figs. 4(a-e) show some profound effect on the morphology of WO_3 particles produced. It is believed with increasing temperature, the diffusion rate increased and this will speed up the coalescence process between neighbouring 'grains' and hence producing larger structures.

For instance, at calcination temperature of 500°C the values is (50 ± 5) nm by Debye-Scherrer formula but (60 – 80) nm with TEM observation The only significant observation was the size by using TEM gave higher measurement than Debye-Scherrer formula. This is due to the fact that XRD measures crystallite size while TEM measures grain size. Grain size is normally bigger that crystallite size as it comprises several crystallite sizes of the particle.

XPS analysis was carried out to examine the electronic binding energy of the sample. Fig. 5(a) is the spectrum for the WO_3 nanoparticles sample at calcination temperature of 400°C. The intensity of the C (Auger) and O (Auger) peaks is high due to the organic molecule residue in the sample even after five times of washing process. Apart from these peaks, no other impurities were detected. Narrow scan for the W_{4f} in Fig. 5(b) shows peaks at 35.8 and 38.0 eV corresponding to the $W_{4f}^{7/2}$ and $W_{4f}^{5/2}$, respectively. While the O_{1s} scan (Fig. 5(c)) shows peaks at 530.8 eV. These results are consistent with the data observed for the binding energy of WO_3 samples [34]. In the study on the XPS, the calcination temperature

at 400°C is chosen since the others gave almost similar results.

5
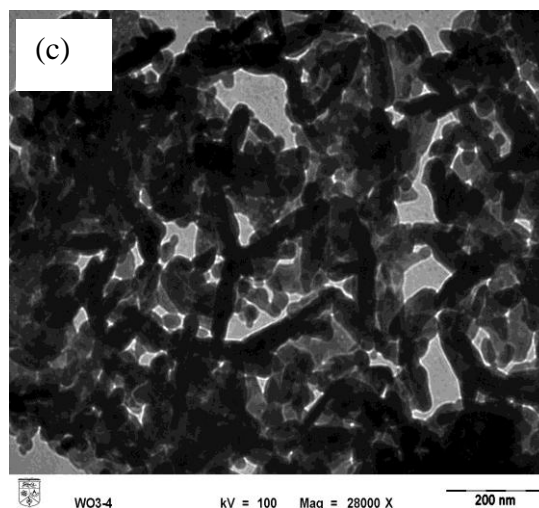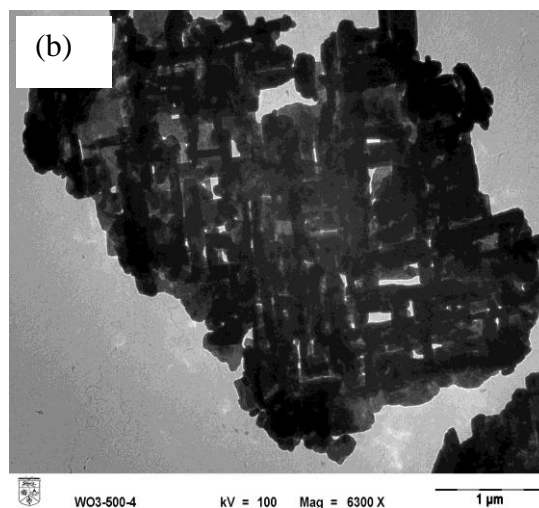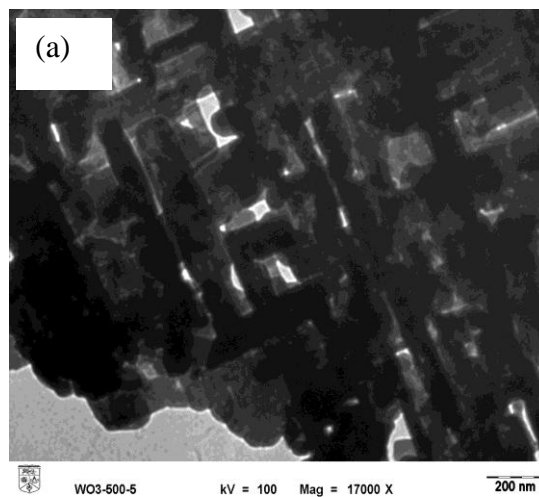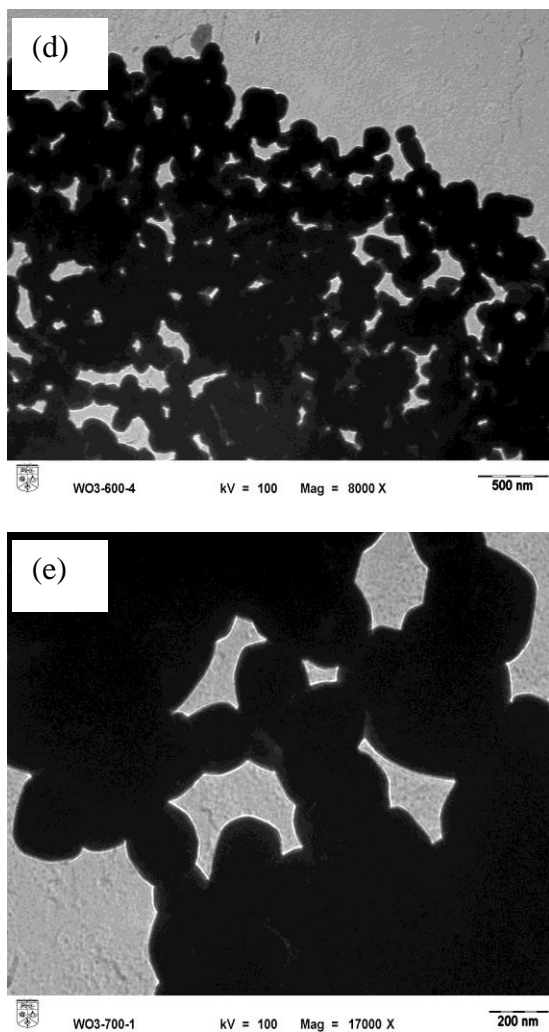
FIG. 4. The TEM images of WO$_3$ nanorods calcined at various temperatures:
(a) as-prepared, (b) 400°C, (c) 500°C, (d) 600°C and (e) 700°C
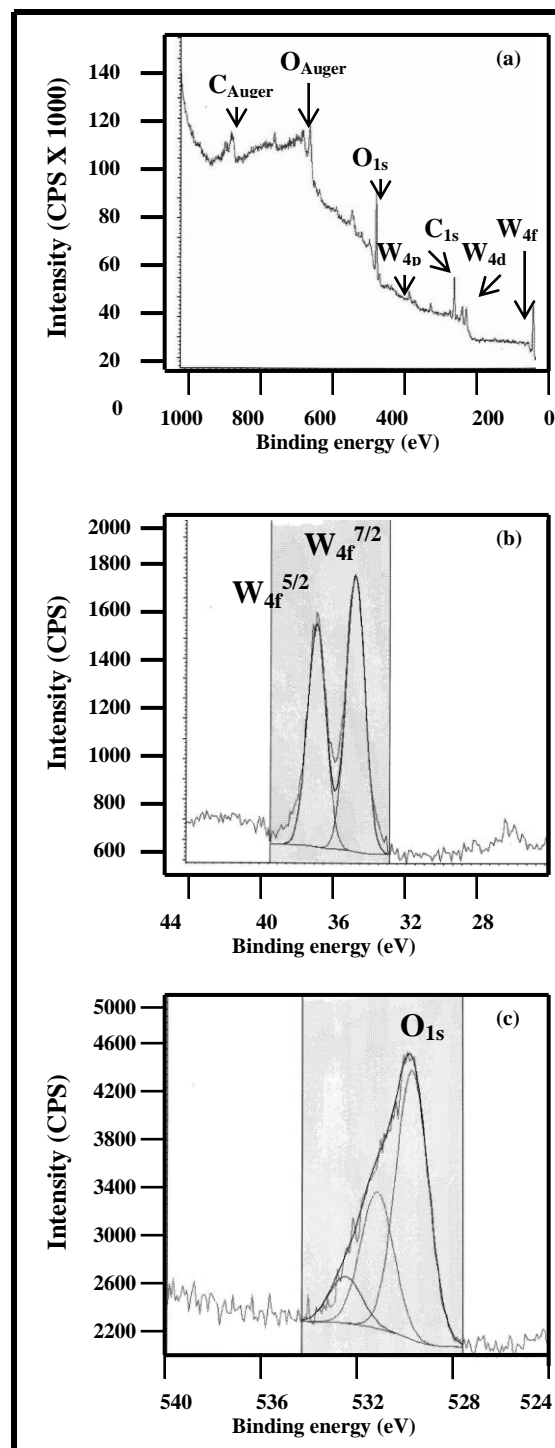
FIG. 5. (a) The wide XPS spectrum of the WO$_3$ nanoparticles at 400°C, (b) narrow scan for W$_{4f}$ peaks and (c) narrow scan for O$_{1s}$ peak.

IV. CONCLUSION

The colloidal gas aphrons system has been developed to produce WO_3 nanoparticles. The increment of particle size and several phase transitions occurred when the WO_3 nanoparticles were heated from 30 to 600°C. The crystallization temperature for WO_3 nanoparticles was found to be above 300°C. The results from XPS show that no significant changes to the composition and the purity of the WO_3 nanoparticles at various calcination temperature. In addition, the nonionic surfactant, Glucopone, that has been employed to form CGAs system in an aqueous solution in this present work is biodegradable and nontoxic to the environment.

REFERENCES

[1] M. Gotic, M. Ivanda, S. Popovic and S. Music. *Mater. Sci. Eng. B* **77** (2000), p. 193.

[2] L.J. Legore, K. Snow, J.D. Galipeau and J.F. Vetelino, *Sens. Actuators B* **35** (1996), p. 164.

[3] Jimenez, J. Arbiol, G. Dezanneau, A. Cornet and J.R. Morante. *Sensors Actuators B* **93** (2003), p. 475.

[4] J.L. Solis, A. Hoel, L.B. Kish, C.G. Granqvist, S. Saukko and V. Lantto. *J. Am. Ceram. Soc.* **84** (2001), p. 1504.

[5] Dutta, N. Kaabbuathong, M.L. Grilli, E. Di Bartolomeo and E. Traversa. *Electrochem. Soc.* **150** (2003), p. H33.

[6] M. Gerlich, S. Kornely, M. Fleischer, H. Meixner and R. Kassing. *Sensors Actuators B* **93** (2003), p. 503.

[7] Jimenez, M.A. Centeno, R. Scotti, F. Morazzoni, A. Cornet and J.R. Morante. *J. Electrochem. Soc.* **150** (2003), p. H72.

[8] R.C. Niall, H.M. Frank, P.H. Bryant. *Optical Materials Technology for Energy Efficiency and Solar Energy Conversion, vol. VI, SPIE.* **823** (1987), p.131.

[9] M. Nabavi, S. Doeuff, C. Sanchez, J. Livage, *Mater. Sci. Eng. B.* **3** (1989), p. 203.

[10] L. Klein. *Sol-Gel Optics: Processing and Applications*. Kluwer, Boston, 1994.

[11] M.P. Pileni. *Langmuir* **13** (1997), p. 3266.

[12] D. Poondi, T. Dobbins, and J. Singh. *J. Mater. Sci.* **35** (2000), p. 6237.

[13] J.G. Lee, J.Y. Park and C.S. Kim. *J. Mater. Sci.* **33** (1998), p. 3965.

[14] X. Mo, C.Y. Wang, M. You, Y.R. Zhu, Z.Y. Chen and Y. Hu. *Mater. Res. Bull.* **36** (1998), p. 2277.

[15] Y. Li, F.Z. Huang, Q.M. Zhang and Z.N. Gu. *J. Mater. Sci.* **35** (2000), p. 5933.

[16] F. Sebba. 1971. *J. Colloid Interface Sci.* **35** (1971), pp. 643.

[17] S.F. Abdullah, S. Radiman, M.A. Abd. Hamid and N.B. Ibrahim, *Colloid Surf. A.* **280** (2006), p. 88.

[18] C. Howard, V. Luca and K. Knight. *J. Phys.: Condens. Matter*. **14** (2002), p. 377.

[19] Y. Xu, S. Carlson and R. Norrestam. *J. Solid State Chem*. **132** (1997), p. 123.

[20] P.M. Woodward, A.W. Sleight and T. Vogt. *J. Solid State Chem*. **131** (1997), p. 9.

[21] K.R. Locherer, I.P. Swainson and E.K.H. Salje. *J. Phys.: Condens. Matter*. **11** (1999), p. 4143.

[22] K.R. Locherer, I.P. Swainson and E.K.H. Salje. *J. Phys.: Condens. Matter*. **11** (1999), p. 6737.

[23] Joint Committee on Powder Diffraction Standards (JCPDS), File No. 71-0131.

[24] Joint Committee on Powder Diffraction Standards (JCPDS), File No. 83-0950.

[25] Joint Committee on Powder Diffraction Standards (JCPDS), File No. 83-0947.

[26] Joint Committee on Powder Diffraction Standards (JCPDS), File No. 75-2072.

[27] J.G. Deng, X.B. Ding, W.C. Zhang, Y.X. Peng, J.H. Wang, X.P. Long, P. Ii and S.C. Chen. *Polymer* **43** (2002), p. 2179.

[28] Yong-Gyu Choi, G. Sakai, K. Shimanoe, N. Miura and N. Yamazoe. *Sensors and Actuators B: Chemical*. **87** (2002), p. 63-72.

[29] E. Salje. *Acta Crystallogr*. A **31** (1975), p. 360.

[30] E. Salje. *Acta Crystallogr*. B **33** (1977), p. 574.

[31] E. Salje and G. Hoppmann. *High Temp. High Pressures*. **12** (1980), p. 213.

[32] E. Cazzanelli, C. Vinegoni, G. Mariotto, A. Kuzmin and J. Purans. *J. Solid State Chem*. **143** (1999), p. 24.

[33] E. Cazzanelli, C. Vinegoni, G. Mariotto, A. Kuzmin and J. Purans. *Solid State Ionics*. **123** (1999), p. 67.

[34] XPS Handbook of The Element and Native Oxides (WO_X) (1999), XPS International, Inc.